Radiative instability in stratified vortices

Stéphane Le Dizès[1] and Paul Billant[2]
[1]*Institut de Recherche sur les Phénomènes Hors Équilibre, CNRS, 49 rue F. Joliot-Curie, F-13013 Marseille, France*
[2]*Laboratoire d'Hydrodynamique (LADHYX), Ecole Polytechnique, F-91120 Palaiseau Cedex, France*

(Received 14 May 2009; accepted 8 September 2009; published online 30 September 2009)

This paper investigates the stability of a columnar vortex in an inviscid stratified fluid. By means of a WKBJ analysis for large axial wave number, we demonstrate that the normal modes can be stable or unstable owing to the emission of internal waves from the vortex. This phenomenon is shown to be analogous to the radioactive decay of nuclei in quantum mechanics. The destabilized character of the wave emission is shown to be associated with the presence of a critical point in the radial structure of the normal mode. The theoretical predictions for the frequency and growth rate of the normal modes are shown to be in good agreement with numerical results for two examples. © *2009 American Institute of Physics*. [doi:10.1063/1.3241995]

I. INTRODUCTION

Inertia-gravity waves are ubiquitous in the rotating stratified flows encountered in geophysics. The spontaneous emission of internal gravity waves from vortices has been predicted for shallow water flows[1] and for strongly stratified rotating fluids.[2] A similar emission of acoustic waves from vortices is observed in compressible fluids[3] or superfluids.[4] This radiative instability has been interpreted in terms of negative energy waves by Kop'ev and Leont'ev.[5] In the physics of the atmosphere, this phenomenon has been associated with wave "over-reflection" at a critical level.[6]

Here, we derive a new and general criterion for the occurrence of the radiative instability in the case of a columnar vortex in a stratified fluid. Our analysis is based on a WKBJ approach for large axial wave number. This approach was also used for the description of a similar instability in the context of accretion disks[7] and shallow water flows.[1,8,9] Here, it will allow us to capture the main characteristics of the eigenmodes and to understand how the radiation of internal waves can be destabilizing.

II. FORMULATION OF THE PROBLEM

We consider an inviscid, incompressible, and stably stratified fluid with constant Brunt–Väisälä frequency N. Under these hypotheses, any vertical axisymmetric vortex with velocity components $\mathbf{U}(r)=[0,V(r),0]$ in cylindrical coordinates (r,θ,z) is steady. We subject this basic flow to infinitesimal three-dimensional perturbations of velocity $\tilde{\mathbf{u}}=(\tilde{u},\tilde{v},\tilde{w})$, pressure $\tilde{p}$, and density $\tilde{\rho}$ written in the form

$$(\tilde{\mathbf{u}},\tilde{p},\tilde{\rho})(r,\theta,z,t)=(\mathbf{u},p,\rho)(r)e^{ikz+im\theta-i\omega t}, \tag{1}$$

where k and m are axial and azimuthal wave numbers and ω is the frequency. Under the Boussinesq approximation (which consists of neglecting density variations everywhere except in the buoyancy force), the linearized equations for these perturbations can be simplified[10] to a single equation for the amplitude $\psi(r)=r^{1/2}G^{-1/2}u(r)$,

$$\frac{d^2\psi}{dr^2}+\frac{k^2(\Phi^2-2\zeta\Omega)}{N^2-\Phi^2}\psi+\left[\frac{m\zeta}{r\Phi}\left(\frac{\zeta'}{\zeta}-\frac{G'}{G}-\frac{2}{r}\right)+\frac{G''}{2G}-\frac{G'}{2rG}-\frac{3}{4}\left(\frac{G'}{G}\right)^2-\frac{3}{4r^2}-\frac{m^2}{r^2}\right]\psi=0, \tag{2}$$

where $\Phi(r)=\omega-m\Omega(r)$ is the Lagrangian frequency, $G(r)=m^2/r^2+k^2\Phi^2/(\Phi^2-N^2)$, and where $\Omega(r)=V/r$ and $\zeta(r)=V'+V/r$ are the angular velocity and the axial vorticity of the vortex. The boundary conditions are that ψ vanishes at the vortex center and corresponds to an outgoing wave at infinity. These conditions applied to the solutions of Eq. (2) define the eigenvalue problem for ω (k and m being fixed).

III. WKBJ ANALYSIS

In Le Dizès and Lacaze,[11] Billant and Gallaire,[10] and Le Dizès,[12] it was shown that a good approximation of the dispersion relation and of the eigenmodes can be obtained by a WKBJ asymptotic analysis for large axial wave number similar to the semiclassical analysis of bounded states in quantum mechanics. For large k, WKBJ approximation of solution to Eq. (2) can be obtained in the following form:

$$\psi(r)\sim Q(r)\left[A\exp\left(i\int^r\beta dy\right)+B\exp\left(-i\int^r\beta dy\right)\right], \tag{3}$$

where A and B are constants and the functions β and Q are given by

$$\beta(r)=k\sqrt{\frac{\Phi^2-2\zeta\Omega}{N^2-\Phi^2}}, \tag{4a}$$

$$Q(r)=\left(\frac{N^2-\Phi^2}{\Phi^2-2\zeta\Omega}\right)^{1/4}. \tag{4b}$$

The square root in β is chosen such that $\Re e(\beta)>0$. The WKBJ approximation (3) breaks down near the so-called turning points where $\beta=0$. However, the different WKBJ approximations on each side of a turning point can be

matched, thanks to standard connection formulas.[13,14] Using this approach, it is thus possible to construct a global WKBJ approximation of the solution over all the integration domain. Enforcing the boundary conditions then yields the dispersion relation.

When the fluid is not stratified ($N=0$) and the vortex centrifugally stable (i.e., $2\zeta\Omega \geq 0$ for all r), Le Dizès and Lacaze[11] showed that eigenmodes can be constructed when there is a finite interval where β^2 is positive. Inside this interval, the WKBJ approximations have an oscillatory behavior while outside they are decaying or growing exponentially. The eigenmodes are called "core" modes when this interval is located between the vortex center and a turning point r_2 and "ring" modes when it is delimited by two turning points r_1 (with $r_1>0$) and r_2. As readily seen from Eq. (4a), the interval where β^2 is positive (i.e., where the WKBJ approximations are oscillatory) for $N=0$ is necessarily located in a region where the vorticity ζ is nonzero, i.e., inside the vortex core.[11] This feature simply reflects the fact that inertial waves are confined to the vortex core. A further condition for the existence of an interval of positive β^2 is that the frequency belongs to the range $\omega^-(r)<\omega<\omega^+(r)$, where

$$\omega^{\pm}(r) = m\Omega(r) \pm \sqrt{2\Omega(r)\zeta(r)}. \tag{5}$$

In contrast, when the fluid is stratified, the regions of positive β^2 are not restricted to the vortex core but can be located everywhere in the fluid. Physically, this is directly related to the fact that two types of waves, inertial waves and internal waves, can exist for a columnar vortex in a stratified fluid. The description of the eigenmodes by a WKBJ approach is therefore expected to be more complex than in the homogeneous case. But, as it will be seen below, the same approach can be used as long as we consider near neutral eigenmodes.

As a first step, we focus here on the strongly stratified case, i.e., the Brunt–Väisälä frequency N is assumed large compared to Ω and ω. This hypothesis implies that the denominator of β^2 in Eq. (4a) is $N^2-\Phi^2 \approx N^2$, i.e., everywhere positive, and that there is no critical point where $\Phi^2=N^2$. The sign of β^2 is then reversed compared to the nonstratified case: β^2 is negative when $\omega^-(r)<\omega<\omega^+(r)$ and positive otherwise.

Figure 1 shows the functions $\omega^+(r)$ and $\omega^-(r)$ for two typical examples:

(1) a hollow vortex: $\Omega(r)=r^2e^{-(r-1)^2}$ for the azimuthal wave number $m=0$ and
(2) a Lamb–Oseen vortex: $\Omega(r)=(1-e^{-r^2})/r^2$ for $m=1$.

Note that these angular velocity profiles are dimensionless. The corresponding dimensional angular velocity is $\hat{\Omega}=\Omega_0\Omega$ and the dimensional radius is $\hat{r}=Rr$, where Ω_0 and R are a typical angular velocity and radius of the vortex. In the following, all the other variables are nondimensionalized accordingly but the same notation is kept. In particular, this means that k corresponds now to the dimensional wave number scaled by the vortex radius and N is now the Brunt–Väisälä frequency divided by Ω_0, i.e., the inverse of a Froude number.

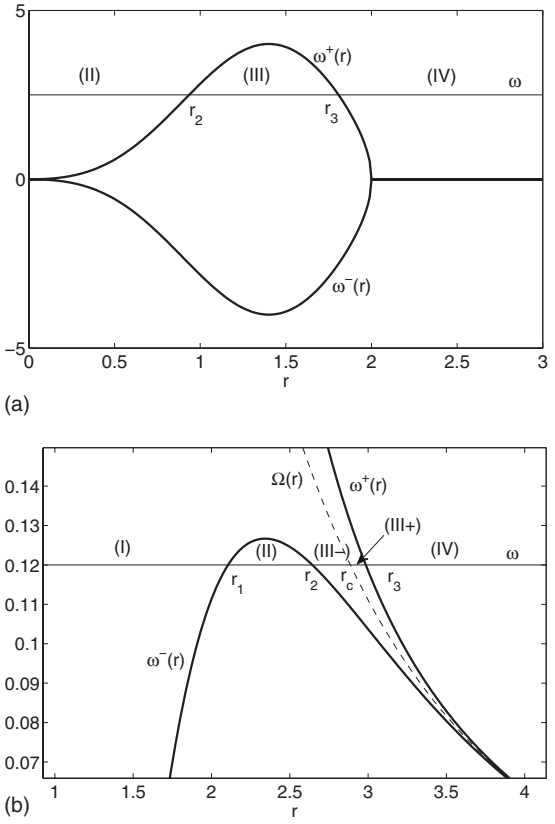

FIG. 1. Variation in the functions ω^+ and ω^- for (a) case (1) and (b) case (2). The different regions and turning points r_i discussed in the text are indicated for a given frequency ω represented by the thin horizontal line. In (b), the critical point r_c has also been indicated.

In each plot of Fig. 1, a particular frequency ω has been indicated by a thin straight line. The comparison of this frequency with $\omega^{\pm}$ gives directly the sign of β^2. For case (1) [Fig. 1(a)], we see that β^2 is positive in the interval between the vortex center and the turning point r_2 (region II) and beyond the turning point r_3 (region IV). Conversely, β^2 is negative for $r_2<r<r_3$ (region III). This configuration occurs for any frequency in the range of $-4<\omega<4$. Case (2) is similar [Fig. 1(b)]: $\beta^2>0$ is positive in the interval $r_1<r<r_2$ (region II) and $r>r_3$ (region IV). Conversely, β^2 is negative for $0<r<r_1$ (region I) and for $r_2<r<r_3$ (region III$\pm$). This configuration is observed for any frequency in the range $0<\omega<0.126$. Case (2) has also another property: there is a critical point r_c between r_2 and r_3 [indicated by the dashed curve in Fig. 1(b)]. This point, defined by $\Phi(r_c)=0$, is a singularity of the equation (2) for that case. The determination of the solution near this point therefore needs a special treatment. We shall see that the presence of the critical point implies that different WKBJ approximations are obtained in the region (III$-$) between r_2 and r_c and in the region (III+) between r_c and r_3.

In cases (1) and (2), there are two intervals of positive β^2: a finite domain in the vicinity of the vortex core (region II) and an infinite domain extending to $+\infty$ (region IV). The goal of the present paper is to show that eigenmodes can be constructed when this situation is encountered. We shall also see the subtle role of the critical point which can make the

eigenmode unstable. Although the two examples chosen above are specific, they are typical of the situations that can occur for any azimuthal wave number m for most vortex profiles in strongly stratified fluids. These two cases are closely related to the core modes and ring modes considered by Le Dizès and Lacaze[11] except that there is an additional outer region of positive β^2 (region IV) where waves can radiate away and a critical point in one of the two cases. For that reason, we shall call them "radiative core modes without critical point" and "radiative ring modes with critical point." As will be explained later, the problem without critical point is in fact analogous to the radioactive decay of bounded states in quantum mechanics: region (II) can be seen as a potential well whereas region (III) plays the role of a potential barrier.

We note that the radiation of waves imposes an imaginary part to the frequency so that β^2 is in fact complex and not purely real as assumed in the discussion above. However, the imaginary part of the frequency will be found to be much smaller than its real part so that the imaginary part of β^2 is always very small. Hence, it is valid to assume β^2 purely real as a first approximation in order to determine the structure of the modes and to consider the imaginary part as a higher order correction. Similarly, throughout the asymptotic analyses, we shall implicitly assume that the eigenfrequencies are real at leading order and that complex corrections are obtained at higher orders.

We now consider in details the two cases (1) and (2).

IV. RADIATIVE CORE MODES WITHOUT CRITICAL POINT

For the case (1) illustrated in Fig. 1(a), the condition that the solution remains bounded at the origin imposes that ψ is given at leading order by (see Le Dizès and Lacaze[11] for details)

$$\psi_{\mathrm{II}}(r) \sim Q(r)\left[\exp\left(i\int_{r_1}^{r}\beta dy\right) + R\exp\left(-i\int_{r_1}^{r}\beta dy\right)\right], \tag{6}$$

with $R=ie^{im\pi}$ and $r_1=0$. In region (IV), the boundary conditions impose that ψ is a wave propagating toward infinity. Since $\partial_\omega\beta>0$ for $r=\infty$, this means that only the wave of radial wave number $+\beta(r)$ should be retained in the general expression (3),[24] i.e.,

$$\psi_{\mathrm{IV}}(r) \sim AQ(r)\exp\left(i\int_{r_3}^{r}\beta dy\right), \tag{7}$$

where A is a constant. The reversible single-turning-point connection formula[14] applied at the turning point r_3 implies that ψ in the "potential barrier" (region III) is given by

$$\psi_{\mathrm{III}}(r) \sim A|Q(r)|\left[\exp\left(\int_{r}^{r_3}|\beta|dy - i\frac{\pi}{4}\right) + \frac{1}{2}\exp\left(-\int_{r}^{r_3}|\beta|dy + i\frac{\pi}{4}\right)\right]. \tag{8}$$

The connection formula at the turning point r_2 gives then another WKBJ approximation inside region (II) (Ref. 14),

$$\psi_{\mathrm{II}'}(r) \sim Ae^{W_{23}}Q(r)\left[\left(1+\frac{e^{-2W_{23}}}{4}\right)\exp\left(i\int_{r_2}^{r}\beta dy\right) - i\left(1-\frac{e^{-2W_{23}}}{4}\right)\exp\left(-i\int_{r_2}^{r}\beta dy\right)\right], \tag{9}$$

with

$$W_{lm} = \int_{r_l}^{r_m}|\beta(r)|dr. \tag{10}$$

Equation (9) shows that the amplitude of the wave reflected at r_2 [second term in the right-hand side (rhs)] is smaller than the incident wave (first term in the rhs). This expression is compatible with Eq. (6) only if

$$-ie^{2iW_{12}}\left(1-\frac{e^{-2W_{23}}}{4}\right) = R\left(1+\frac{e^{-2W_{23}}}{4}\right). \tag{11}$$

When the potential barrier is large, i.e., when $\epsilon = \exp(-2W_{23}) \ll 1$, this condition can be expanded with the small parameter ϵ. Writing the frequency in the form $\omega = \omega_0 + \delta\omega + \cdots$ with $\delta\omega = O(\epsilon)$ leads at leading order in ϵ to the same discretization rule as for nonradiative core modes (Le Dizès and Lacaze[11]),

$$\int_0^{r_2}\beta(r)dr = \frac{|m|\pi}{2} + n\pi, \tag{12}$$

where n is a non-negative integer. This relation gives the leading order frequency ω_0. The next order in ϵ yields the frequency correction due to the wave emission through the potential barrier

$$\delta\omega = -\frac{i}{4}\frac{\exp(-2W_{23})}{\int_{r_1}^{r_2}\partial\beta/\partial\omega dr}. \tag{13}$$

It is worth mentioning that Eq. (13) is based on the use of reversible connection formula[14] which amounts to keep the decreasing exponential even in the presence of an increasing exponential. As discussed by Shepard,[14] even if there is a long-standing controversy, this generally leads to meaningful and reliable results. In the present case, it gives the leading frequency correction due to the sole wave emission.

V. RADIATIVE RING MODES WITH CRITICAL POINT

Case (2) which leads to radiative ring modes is similar to the one considered above except that there exists an additional region (I) in the vicinity of the vortex axis and a critical point within the region (III) [Fig. 1(b)]. Near the origin, the solution of Eq. (2) which remains finite for $r=0$ is the Bessel function I_m, which behaves like $I_m(x) \sim e^x/\sqrt{2\pi x}$ for large x. This implies that the WKBJ approximation in region (I) is

$$\psi_I(r) \sim B|Q(r)|\exp\left(\int_0^r |\beta| dy\right), \tag{14}$$

where B is a constant. The connection formula at the turning point r_1 leads to a solution in region (II) of the same form as Eq. (6) but with $R=i$. The solutions in regions (III+) and (IV) are identical to Eqs. (8) and (7). However, owing to the presence of the critical point r_c, an expression different from Eq. (8) has to be used in region (III−). This expression has been obtained in the Appendix. It leads to a new expression in region (II) which replaces Eq. (9),

$$\psi_{II'}(r) \sim Ae^{W_{23}}Q(r)\left[\left(\mu_2 - \frac{ae^{-2W_{c3}}}{2} - \frac{ae^{-2W_{2c}}}{2} + \mu_1\frac{e^{-2W_{23}}}{4}\right)\exp\left(i\int_{r_2}^r \beta dy\right) - i\left(\mu_2 - \frac{ae^{-2W_{c3}}}{2} + \frac{ae^{-2W_{2c}}}{2} - \mu_1\frac{e^{-2W_{23}}}{4}\right)\exp\left(-i\int_{r_2}^r \beta dy\right)\right], \tag{15}$$

where W_{lm} has been defined in Eq. (10), $a=\pi/(2|\beta_c|k)$ with β_c being the value of β at r_c and μ_i are constants such that $\mu_i=1+O(1/k)$. A slightly different compatibility condition is then obtained,

$$-ie^{2iW_{12}}\left(\mu_2 - \frac{ae^{-2W_{c3}}}{2} + \frac{ae^{-2W_{2c}}}{2} - \mu_1\frac{e^{-2W_{23}}}{4}\right) = R\left(\mu_2 - \frac{ae^{-2W_{c3}}}{2} - \frac{ae^{-2W_{2c}}}{2} + \mu_1\frac{e^{-2W_{23}}}{4}\right). \tag{16}$$

Since $e^{-2W_{23}}, a, e^{-2W_{c3}}, e^{-2W_{2c}}$ are *a priori* all small and $\mu_i \approx 1$, we deduce at leading order the same discretization rule as for nonradiative ring modes,[11]

$$\int_{r_1}^{r_2} \beta(r) dr = \left(n+\frac{1}{2}\right)\pi, \tag{17}$$

showing that the critical point has no effect at leading order. However, the frequency correction at next order contains a term generated by the critical point

$$\delta\omega = -\frac{i}{4}\frac{e^{-2W_{23}} - 2ae^{-2W_{2c}}}{\int_{r_1}^{r_2}\partial\beta/\partial\omega dr}. \tag{18}$$

Note that Eq. (13) is recovered if $a=0$. *A priori*, Eq. (18) applies when the three points r_2, r_c, and r_3 are far from each other. For case (2), we shall see in Sec. VII that a better estimate can be obtained by considering that three points r_2, r_c, and r_3 are merged to a single point.

VI. ANALOGY WITH THE RADIOACTIVE DECAY IN QUANTUM MECHANICS

The above formulas (17) and (13) have exact analogs in quantum mechanics in the case of the radioactive decay of bounded states. In that case, the governing equation is the Schrödinger equation for the wave function amplitude ψ of a particle of mass m and energy E,

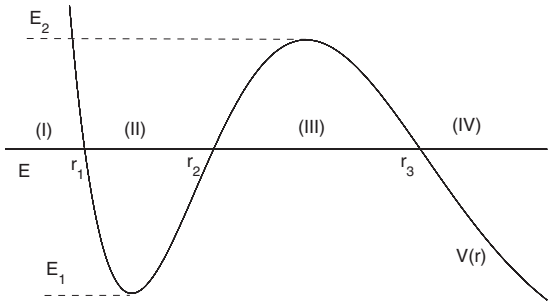

FIG. 2. Typical potential exhibiting bounded states and radioactive decay.

$$\frac{\hbar^2}{2m}\frac{\partial^2\psi}{\partial r^2} + [E - V(r)]\psi = 0, \tag{19}$$

where $\hbar$ is the Planck's constant and $V(r)$ is the potential. WKBJ analyses performed in the semiclassical limit $\hbar \to 0$ for a potential V with the typical shape displayed in Fig. 2 show that the energy levels of the "bounded states" (i.e., with $E_1 < E < E_2$) are given by the well-known *Bohr–Sommerfeld* quantization rule.[15] This relation is identical to Eq. (17) except that β is given by

$$\beta(r) = \frac{\sqrt{2m}}{\hbar}\sqrt{E - V(r)}.$$

As the Schrödinger equation does not possess critical points, the decay rate due to the radioactivity across the potential barrier is given by Eq. (13) with ω replaced by E. This formula was first obtained by Gamow[16] to explain the alpha emission by atoms. A more recent account can also be found in Shepard.[14]

VII. DOUBLE-TURNING-POINT ANALYSIS

Formulas (17) and (18) obtained above for case (2) assume that the three points r_2, r_c, and r_3 are well separated. When $\omega/m \sim 1/\log(k/N)$, the three points become separated by a distance of order $\log(k/N)/\sqrt{k/N}$ and formulas (17) and (18) break down. In this section, we are going to show that a better estimate can be obtained by assuming that the three points are merged at leading order. This occurs when $\omega \ll 1/\log(k/N)$. In this case, the three points are located at $r_t = \sqrt{m/\omega}$ where the vorticity is $o(N/k)$, and Eq. (2) reduces at leading order in k/N near r_t to

$$\frac{\partial^2\psi}{\partial\tilde{r}^2} + \left[4\tilde{r}^2 - \frac{2}{\tilde{r}^2}\right]\psi = 0 + O\left(\frac{N^{1/2}}{k^{1/2}\omega^{1/4}}\right), \tag{20}$$

with $\tilde{r} = \sqrt{\lambda}(r - r_t)$ and $\lambda = |k\Phi'(r_t)/(2N)|$. As seen from the neglected order, this equation also requires ω not to be too small: $\omega \gg (N/k)^2$. The solution which matches the outgoing wave (7) in region (IV) for $\tilde{r} \to +\infty$ is $\psi(\tilde{r}) = B\tilde{r}^{1/2}H^{(1)}_{3/4}(\tilde{r}^2)$, where $B = A\sqrt{\pi k}e^{5i\pi/8}/(2\lambda^{1/4})$ and $H^{(1)}_{3/4}$ is the Hankel function of the first kind. From the behavior of the Hankel function $H^{(1)}_{3/4}(z)$ for $|z| \to \infty$ with $\arg(z) = 2\pi$, one can deduce the valid WKBJ approximation in region (II),

$$\psi_{\mathrm{II}'} \sim AQ(r)\left[\sqrt{2}\exp\left(i\int_{r_2}^{r}\beta dy\right)+i\exp\left(-i\int_{r_2}^{r}\beta dy\right)\right]. \tag{21}$$

By comparing Eqs. (21) and (6) we deduce a modified relation for case (2),

$$\int_{r_1}^{r_2}\beta(r)dr = n\pi - \frac{i\ln(2)}{4}, \tag{22}$$

which is valid for ω satisfying $(N/k)^2 \ll \omega \ll 1/\log(k/N)$.

When $\omega=0$, region (II) extends to infinity (i.e., $r_t=\infty$). Then, the solution of Eq. (2) can be found analytically for $r \gg 1$ in the form

$$\psi = \frac{A}{r^{3/2}G^{1/2}}J'_m\left(\frac{k|m|}{Nr}\right), \tag{23}$$

where A is a constant, J_m the Bessel function of the first kind and where only the solution which decays as $r\to\infty$ has been retained. Assuming $k \gg 1$ in Eq. (23) gives the valid WKBJ approximation in region (II),

$$\psi_{\mathrm{II}'} \sim BQ(r)\left[\exp\left(i\int_{\infty}^{r}\beta dy\right) + i\exp\left(-i|m|\pi - i\int_{\infty}^{r}\beta dy\right)\right], \tag{24}$$

where B is a constant. Matching Eqs. (24) and (6) gives the discretization rule

$$\int_{r_1}^{\infty}\beta(r)dr = \frac{|m|\pi}{2} + n\pi, \tag{25}$$

which is valid only for $\omega=0$.

VIII. NUMERICAL COMPARISON

The above formulas are tested for $N=5$ in Fig. 3 for case (1) and in Fig. 4 for case (2). The numerical results, which are shown by open circles, have been obtained by a shooting method. The critical points, when they are present as in case (2), are avoided by deforming the integration contour in the complex plane. In case (1), the integration contour also ends in the complex plane (along a line $r=se^{i\phi}$ with typically $\phi=\pi/10$) such that the damped eigenmodes remain bounded at infinity. This trick strongly speeds up the numerical algorithm without modifying the eigenvalues.

As for normal modes without wave emission,[11] the real part of the frequency is very well predicted by the discretization formula (12) for case (1) [solid lines in Fig. 3(a)]. Surprisingly, the branches continue up to $\omega=N=5$, i.e., above the maximum of ω^+. This corresponds to modes "above the potential barrier." It turns out that the frequency and damping rate of such modes can be obtained by applying formula (12) in the complex plane (see the dashed lines in Fig. 3) as explained in Le Dizès and Lacaze.[11]

For case (2), we have tested formulas (17) and (18) obtained for distant turning points and formula (22) obtained for a double-turning point. We have observed that the first

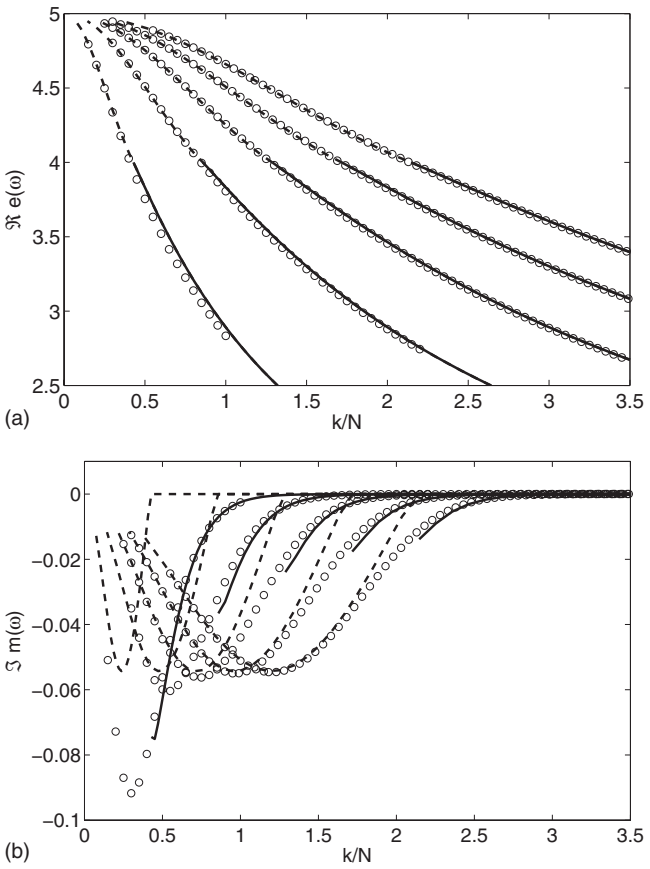

FIG. 3. (a) Frequency $\Re e(\omega)$ and (b) growth rate $\Im m(\omega)$ for case (1) for $N=5$. Solid line: WKBJ formula (12) for $\Re e(\omega)$ and Eq. (13) for $\Im m(\omega)$; dashed line: formula (12) applied in the complex plane. Symbols: numerical results. Only the five first branches have been plotted.

formulas (17) and (18) do not provide good predictions of the numerical results for the axial wave numbers that we have considered. By contrast, the formula (22) predicts well the frequency of the modes for $k/N<60$ [solid lines in Fig. 4(a)] except the first branch which becomes damped around $k/N=6$ and is not captured by the large-k asymptotic analysis. In fact, this branch is specific since it derives from a displacement mode for $k\to 0$. We can also notice in Fig. 4(a) that the frequency predicted by Eq. (22) departs from the numerical results around $\omega=0$. This is not surprising as Eq. (22) is only valid for $\omega \gg (N/k)^2$. The specific formula (25) for $\omega=0$ is indicated by black squares and can be seen to be in very good agreement with the numerical results except for the first branch. In practice, a very good agreement for all the frequency can be obtained by using the empirical formula

$$\int_{r_1}^{r_2}\beta(r)dr = \frac{|m|\pi}{2} + n\pi, \tag{26}$$

together with the frequency correction

$$\delta\omega = -\left[\frac{|m|\pi}{2} + \frac{i\ln(2)}{4}\right] \Big/ \int_{r_1}^{r_2}\partial_\omega\beta dr. \tag{27}$$

These formulas can be seen as an empirical "composite" approximation: they tend to Eq. (25) for $\omega\to 0$ and to Eq. (22)

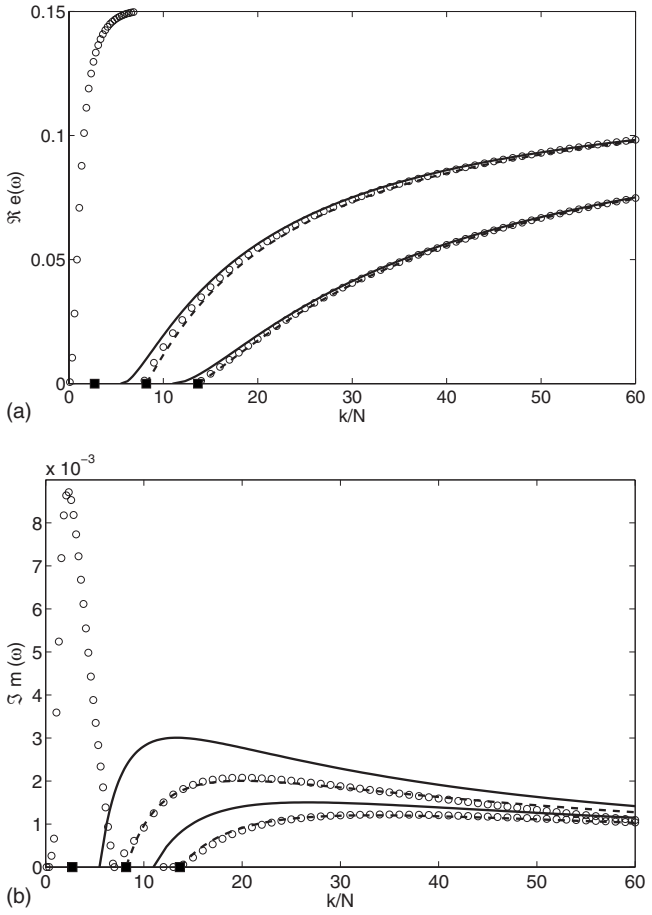

FIG. 4. [(a) and (b)] Same as Fig. 3 for case (2) and $N=5$ except that formula (22) has been used to plot the solid lines. The dashed lines show the predictions obtained from Eqs. (26) and (27). The black squares show the results of the formula (25). Only the three first branches have been plotted.

for finite ω. They are represented by the dashed lines in Fig. 4.

Remarkably, the growth rates plotted in Figs. 3(b) and 4(b) show that the normal modes for case (1) are stable while they are unstable for case (2). Formula (13) for case (1) predicts very well the damping rate of the modes. For case (2), Eq. (22) predicts also reasonably well the growth rate of the modes, the first branch excepted [Fig. 4(b)]. However, as seen by the dashed lines, a much better agreement is obtained by using Eqs. (26) and (27).

IX. INSTABILITY MECHANISM

It is quite striking that the wave emission is stabilizing for case (1) as for the radioactive decay of nuclei, while it is destabilizing for case (2). The origin of this difference can be understood by looking at the sign of $\partial_\omega \beta$ in region (II) since it controls directly the sign of the growth rate [i.e., $\Im m(\delta\omega)$] in Eqs. (13) and (27). Physically, the sign of $\partial_\omega \beta$ defines locally the direction of propagation of energy. Since $\partial_\omega \beta = (k/N)\Phi/\sqrt{\Phi^2 - 2\zeta\Omega}$ for a strongly stratified fluid, it is itself directly given by the sign of the local Lagrangian frequency $\Phi(r) = \omega - m\Omega(r)$. For case (2), this quantity changes sign at the critical point r_c in region (III). Therefore, $\partial_\omega \beta$ is of opposite sign in regions (II) and (IV) in case (2) whereas it keeps the same sign in case (1). For case (2), this implies that the wave which propagates energy outward ($\partial_\omega \beta > 0$) in region (IV) transforms to a wave propagating energy inward ($\partial_\omega \beta < 0$) in region (II). In other words, the potential barrier (region III) plays the role of an energy source which transfers energy to both the bounded states (region II) and to the radiated wave (region IV). This explains why the internal wave radiation is destabilizing when there is a critical point as in case (2) and stabilizing when there is no critical point as in case (1). A quite similar explanation, based on the concept of wave action, was also provided in Narayan *et al.*[7] in the context of accretion disks. Case (2) can also be viewed as a configuration with over-reflection: the wave propagating energy in region (II) toward region (III), which corresponds to the second wave in Eq. (21), has a smaller amplitude than the reflected wave. As in Lindzen and Barker,[6] we have seen that a critical point is also necessary for this over-reflection process. Note, however, that the role of the critical point is quite subtle. When the potential barrier becomes large, we have to use expression (18) for the growth rate instead of Eq. (27). As the second term of this expression can become dominant, we may no longer be unstable. This restabilization can be understood by the same arguments. In that case, the dominant effect on the waves emitted toward region (IV) by the bounded state leaving in region (II) is the absorption and reflection at the critical point r_c. There is no longer over-reflection as the reflected wave has now a smaller amplitude than the incident wave [see expression (15)]. This dual effect of the critical point has also been pointed out by Schecter and Montgomery.[2]

X. CONCLUSION

We have demonstrated that the emission of internal waves by columnar vortices in strongly stratified fluid can be described for large axial wave number by similar WKBJ formulas as those for the radioactive decay of bounded states in quantum mechanics. These formulas explain the discretization of the frequencies of the normal modes and provide the growth rate due to the wave radiation. In contrast to the radioactive decay, the wave emission can be destabilizing owing to the presence of a critical point in the potential barrier where the direction of energy propagation is reversed. When the potential barrier is infinitely thin, we have seen that the growth rate of the instability is the largest and that it is proportional to the wave transmission coefficient across the potential barrier. By contrast, for finite potential barriers, the destabilizing effect of the wave emission becomes exponentially small and can be dominated by the stabilizing absorption at the critical point.

When the rotating flow is confined between two boundaries, another instability generated by the stratification is possible as observed in Taylor–Couette flows in centrifugally stable regimes.[17,18] The instability mechanism is, however, different from that described in the present paper, as it is due to the resonance of two modes localized near each boundary.[19] A WKBJ description of this instability would be interesting as already done for shallow-water flows,[8,20] strongly rotating shear flows,[21] and accretion disks.[7]

APPENDIX: ANALYSIS OF THE CRITICAL POINT REGION

In this section, we consider the problem around the critical point in order to determine the modifications that this point induces on the WKBJ approximations in region (III−) of case (2) [see Fig. 1(b)]. For this purpose, it is convenient to consider the problem for the pressure p which satisfies the equation

$$\frac{d^2p}{dr^2}+\left(\frac{1}{r}-\frac{\Delta'}{\Delta}\right)\frac{dp}{dr}+\left[\frac{2m}{r\Phi\Delta}(\Omega\Delta'-\Omega'\Delta)+\frac{k^2\Delta}{\Phi^2-N^2}-\frac{m^2}{r^2}\right]p=0, \tag{A1}$$

with

$$\Phi(r)=\omega-m\Omega(r),\quad \Delta(r)=2\zeta(r)\Omega(r)-\Phi^2(r). \tag{A2}$$

An expression for ψ can then be deduced from p by the relation

$$\psi=\left(\frac{r}{G}\right)^{1/2}\left(\frac{i\Phi}{\Delta}\frac{\partial p}{\partial r}-\frac{2im\Omega}{r\Delta}p\right). \tag{A3}$$

The problem is the following. Without critical point, WKBJ approximations are uniformly valid in region (III). This means that if we consider two WKBJ expressions of p,

$$p_{\mathrm{III}\pm}\sim P(r)[S^{\pm}e^{-|\int_{r_c}^{r}\beta dy|}+D^{\pm}e^{|\int_{r_c}^{r}\beta dy|}], \tag{A4}$$

where the sign + or − denotes $r>r_c$ and $r<r_c$, respectively, and $P(r)=\Delta^{1/4}(N^2-\Phi^2)^{1/4}r^{-1/2}$, the coefficients $C^-=(S^-,D^-)^{\perp}$ and $C^+=(S^+,D^+)^{\perp}$ are connected with each other by a reversible connection relation $C^{\pm}=M_pC^{\mp}$ with a matrix M_p defined by

$$M_p=\begin{pmatrix}0 & 1\\ 1 & 0\end{pmatrix}. \tag{A5}$$

If r_c is a critical point, we are going to show that a different relation applies, which is obtained by studying the neighborhood of r_c. The analysis of the solution near a critical point r_c, defined by $\Phi(r_c)=0$, is performed by expanding Eq. (A1) near r_c and by searching for a local solution, say $\tilde{p}$ as a function of a local variable $\tilde{r}=k(r-r_c)$. Up to $O(1/k^2)$ terms, we obtain that $\tilde{p}(\tilde{r})$ satisfies

$$\tilde{p}''-|\beta_c|^2\tilde{p}+\frac{1}{k}\left(\frac{1}{r_c}-\frac{\Delta_c'}{\Delta_c}\right)\tilde{p}'-\left[\frac{\Delta_c'\tilde{r}}{N^2}+\frac{2}{r_c\Omega_c'\Delta_c\tilde{r}}(\Omega_c\Delta_c'-\Omega_c'\Delta_c)\right]\tilde{p}=0, \tag{A6}$$

where the index c indicates values taken at r_c. The general solution of this equation is

$$\tilde{p}(\tilde{r})=A_0\left[e^{|\beta_c|\tilde{r}}\left(1+\frac{\mu\tilde{r}}{k}+\frac{\lambda\tilde{r}^2}{k}\right)+\frac{\gamma}{k}e^{-|\beta_c|\tilde{r}}\int_{-\infty}^{\tilde{r}}e^{2|\beta_c|u}\log(u)du\right]+B_0\left[e^{-|\beta_c|\tilde{r}}\left(1+\frac{\mu\tilde{r}}{k}-\frac{\lambda\tilde{r}^2}{k}\right)+\frac{\gamma}{k}e^{|\beta_c|\tilde{r}}\int_{\infty}^{\tilde{r}}e^{-2|\beta_c|u}\log(u)du\right], \tag{A7}$$

with

$$\mu=-\frac{1}{2r_c}+\frac{\Delta_c'}{4\Delta_c},\quad \lambda=\frac{\Delta_c'}{4N^2|\beta_c|},\quad \gamma=\frac{2\Omega_c\zeta_c'}{r_c\Omega_c'\zeta_c}. \tag{A8}$$

In the above integrals, the branch cut of the logarithm is chosen along the negative real axis. The integration path is prescribed by the condition that the solution should become uniformly valid on the real axis when a small positive imaginary part is added to the frequency. When $m>0$ and $\Omega_c'<0$, as in case (2), this condition implies that the integration path is "above" the branch cut, that is $-\infty=|\infty|e^{i\pi}$. Note, however, that the logarithm singularity is still present as $\tilde{r}\to 0$. This singularity, which corresponds to the critical layer singularity, requires additional effects to be smoothed. Assuming that the solution remains valid on the integration path mentioned above, that is above the singularity in the complex plane, means that the singularity is smoothed by viscous effects as explained by the classical theory of viscous critical layers.[22]

In order to obtain the connection formula across r_c, we need to determine the behavior of $\tilde{p}(\tilde{r})$ when $\tilde{r}\to\pm\infty$. The problem then reduces to an evaluation of the behavior of the functions

$$f^{\pm}(\tilde{r})=e^{\pm|\beta_c|\tilde{r}}\int_{\pm\infty}^{\tilde{r}}e^{\mp 2|\beta_c|u}\log(u)du \tag{A9}$$

for large $|\tilde{r}|$.

There is no difficulty to evaluate f^+ at $+\infty$ and f^- at $-\infty$ as they are both subdominant. The difficulty is to compute the subdominant contribution to $f^{\pm}$ when they become exponentially large. Let us consider $f^+(\tilde{r})$. A similar method can be used for $f^-(\tilde{r})$. The idea is to perform an integration by part,

$$f^+(\tilde{r})=-e^{-|\beta_c|\tilde{r}}\frac{\log(\tilde{r})}{2|\beta_c|}+\frac{e^{|\beta_c|\tilde{r}}}{2|\beta_c|}\int_{+\infty}^{\tilde{r}}\frac{e^{-2|\beta_c|u}}{u}du, \tag{A10}$$

such that the subdominant contribution that is created as $\tilde{r}\to-\infty$ becomes apparent. It comes from the pole singularity of the second integral and can be computed by "residue theorem." It leads to the following behavior of $f^+(\tilde{r})$ as $\tilde{r}\to-\infty$:

$$f^+(\tilde{r})\underset{\tilde{r}\to-\infty}{\sim}-\frac{e^{-|\beta_c|\tilde{r}}}{2|\beta_c|}[\log(|\tilde{r}|)+O(1)]+\frac{i\pi}{2|\beta_c|}e^{|\beta_c|\tilde{r}}, \tag{A11}$$

where the subdominant contribution is the second part of this expression. Similarly, we obtain for $f^-(\tilde{r})$ as $\tilde{r}\to+\infty$,

$$f^-(\tilde{r}) \underset{\tilde{r}\to+\infty}{\sim} \frac{e^{|\beta_c|\tilde{r}}}{2|\beta_c|}[\log(\tilde{r}) + O(1)] + \frac{i\pi}{2|\beta_c|}e^{-|\beta_c|\tilde{r}}. \tag{A12}$$

From these expressions, we can obtain the behavior of $\tilde{p}$ as $\tilde{r}\to\pm\infty$,

$$\tilde{p} \underset{\tilde{r}\to+\infty}{\sim} A_0\left\{e^{|\beta_c|\tilde{r}}[1+O(1/k)] + \frac{i\pi}{2|\beta_c|k}e^{-|\beta_c|\tilde{r}}[1+O(1/k)]\right\} + B_0 e^{-|\beta_c|\tilde{r}}[1+O(1/k)], \tag{A13}$$

$$\tilde{p} \underset{\tilde{r}\to-\infty}{\sim} A_0 e^{|\beta_c|\tilde{r}}[1+O(1/k)] + B_0\left\{e^{-|\beta_c|\tilde{r}}[1+O(1/k)] + \frac{i\pi}{2|\beta_c|k}e^{|\beta_c|\tilde{r}}[1+O(1/k)]\right\}, \tag{A14}$$

from which we can deduce the matrix M_p that connects the coefficients $C^-=(S^-,D^-)^\perp$ and $C^+=(S^+,D^+)^\perp$ of the WKBJ approximations across r_c,

$$M_p = \begin{pmatrix} ia & \mu_1 \\ \mu_2 & -ia \end{pmatrix}, \quad a = \frac{\pi}{2|\beta_c|k}, \tag{A15}$$

where μ_i are coefficients such that $\mu_i = 1+O(1/k)$.

The connection formula across r_c for the function ψ can then be easily deduced by using Eq. (A3). We obtain the connection matrix

$$M_\psi = \begin{pmatrix} -ia & \mu_1 \\ \mu_2 & ia \end{pmatrix}. \tag{A16}$$

We are now in a position to determine the effect of the critical point on the solution of case (2). For case (2), the critical point modifies the WKBJ approximations in region (III−). The approximation in region (III+) is still given by Eq. (8) as this expression is obtained by the condition of radiation in region (IV). This expression can also be written as

$$\psi_{\mathrm{III}+}(r) \sim A|Q(r)|\left[e^{W_{c3}}e^{-|\int_{r_c}^r|\beta|dy|}e^{-i(\pi/4)} + \tfrac{1}{2}e^{-W_{c3}}e^{|\int_{r_c}^r|\beta|dy|}e^{i(\pi/4)}\right]. \tag{A17}$$

Using the above expression for M_ψ, we deduce the expression in region (III−),

$$\psi_{\mathrm{III}-} \sim A|Q(r)|e^{i(\pi/4)}\left[\left(-ae^{W_{c3}} + \frac{\mu_1}{2}e^{-W_{c3}}\right)e^{-|\int_{r_c}^r|\beta|dy|} + i\left(\frac{a}{2}e^{-W_{c3}} - \mu_2 e^{W_{c3}}\right)e^{|\int_{r_c}^r|\beta|dy|}\right], \tag{A18}$$

from which we can obtain expression (15) for the solution in region (II) by using the connection formula across a single turning point.[14]

[1] R. Ford, "The instability of an axisymmetric vortex with monotonic potential vorticity in rotating shallow water," J. Fluid Mech. **280**, 303 (1994).
[2] D. A. Schecter and M. T. Montgomery, "Damping and pumping of a vortex Rossby wave in a monotonic cyclone: Critical layer stirring versus inertia-buoyancy wave emission," Phys. Fluids **16**, 1334 (2004).
[3] E. G. Broadbent and D. W. Moore, "Acoustic destabilization of vortices," Philos. Trans. R. Soc. London, Ser. A **290**, 353 (1979).
[4] P. H. Roberts, "On vortex waves in compressible fluids. I. The hollow-core vortex," Philos. Trans. R. Soc. London, Ser. A **459**, 331 (2003).
[5] V. F. Kop'ev and E. A. Leont'ev, "Acoustic instability of an axial vortex," Sov. Phys. Acoust. **29**, 111 (1983).
[6] R. S. Lindzen and J. W. Barker, "Instability and wave over-reflection in stably stratified shear flow," J. Fluid Mech. **151**, 189 (1985).
[7] R. Narayan, P. Goldreich, and J. Goodman, "Physics of modes in a differentially rotating system–analysis of the shearing sheet," Mon. Not. R. Astron. Soc. **228**, 1 (1987).
[8] N. J. Balmforth, "Shear instability in shallow water," J. Fluid Mech. **387**, 97 (1999).
[9] D. G. Dritschel and J. Vanneste, "Instability of a shallow-water potential-vorticity front," J. Fluid Mech. **561**, 237 (2006).
[10] P. Billant and F. Gallaire, "Generalized Rayleigh criterion for nonaxisymmetric centrifugal instabilities," J. Fluid Mech. **542**, 365 (2005).
[11] S. Le Dizès and L. Lacaze, "An asymptotic description of vortex Kelvin modes," J. Fluid Mech. **542**, 69 (2005).
[12] S. Le Dizès, "Inviscid waves on a Lamb–Oseen vortex in a rotating stratified fluid: Consequences for the elliptic instability," J. Fluid Mech. **597**, 283 (2008).
[13] C. M. Bender and S. A. Orszag, *Advanced Mathematical Methods for Scientists and Engineers* (McGraw-Hill, New York, 1978).
[14] H. K. Shepard, "Decay widths for metastable states. Improved WKB approximation," Phys. Rev. D **27**, 1288 (1983).
[15] L. Landau and E. Lifchitz, *Mécanique Quantique, Théorie Non Relativiste* (Mir, Moscow, 1967).
[16] G. Gamow, "Zur Quantentheorie des Atomkernes," Z. Phys. **51**, 204 (1928).
[17] M. J. Molemaker, J. C. McWilliams, and I. Yavneh, "Instability and equilibration of centrifugally stable stratified Taylor–Couette flow," Phys. Rev. Lett. **86**, 5270 (2001).
[18] M. Le Bars and P. Le Gal, "Experimental analysis of the stratorotational instability in a cylindrical Couette flow," Phys. Rev. Lett. **99**, 064502 (2007).
[19] I. Yavneh, J. McWilliams, and M. J. Molemaker, "Non-axisymmetric instability of centrifugally stable stratified Taylor–Couette flow," J. Fluid Mech. **448**, 1 (2001).
[20] C. Knessl and J. B. Keller, "Stability of rotating shear flows in shallow water," J. Fluid Mech. **244**, 605 (1992).
[21] J. Vanneste and I. Yavneh, "Unbalanced instabilities of rapidly rotating stratified shear flows," J. Fluid Mech. **584**, 373 (2007).
[22] C. C. Lin, *The Theory of Hydrodynamics Stability* (Cambridge University Press, Cambridge, 1955).
[23] J. A. Spiers, "On the escape of a particle from a potential well," J. Phys. A **13**, 2049 (1980).
[24] Note that when $\Im m(\omega)<0$, the wave propagating energy outward is such that $\Im m(\beta)<0$, which implies that ψ increases exponentially with r. This behavior is not unphysical, if one thinks that at $t=0$, the wave field begins to travel outward from the vortex center at a finite velocity [see also the discussion in Roberts (Ref. 4) and Spiers (Ref. 23)].